Journal of Computational Science and Technology

Vol. 5, No. 1, 2011

New Surrogate Model to Predict Fracture of Laminated CFRP for Structural Optimization*

Akira TODOROKI**, Takashi SHINODA***, Yoshihiro MIZUTANI**** and Ryosuke MATSUZAKI****

**Department of Mechanical Sciences and Engineering, Tokyo Institute of Technology
2-12-1 Ookayama, Meguro-ku, Tokyo 152-8552, Japan
E-mail:atodorok@ginza.mes.titech.ac.jp

*** Tokyo Institute of Technology

**** Department of Mechanical Sciences and Engineering, Tokyo Institute of Technology
2-12-1 Ookayama, Meguro-ku, Tokyo 152-8552, Japan

Abstract

Laminated composite structures are widely used for aerospace components because of their high specific strength and specific stiffness. For laminated composite structures, stacking sequence optimization is indispensable. Although fracture of the laminated composites is usually used as a constraint, it is very important to obtain an accurate approximation of the fracture of the laminated composites for the optimization of surrogate models. Approximating the fracture of laminated composites, however, is quite difficult because the fracture index is very noisy. In the present study, a new surrogate model using the Kriging model for the fracture of laminated composites is proposed and tested for the most severe plate bending problems.

Key words: Optimization, Composite, Fracture, Response Surface, Kriging

1. Introduction

Laminated Carbon Fiber Reinforced Polymer (CFRP) composites have been widely adopted for aerospace structural components to save on weight. Since the laminate CFRP composites have strong anisotropic properties, the CFRP composite structures require optimal design of the stacking sequences as well as optimal design of the dimensions of the components. Miki [(1)] and Fukunaga [(2)] both proposed a graphical optimization method using the lamination parameters. For practical laminated CFRP structures, however, the available fiber angles are limited to a small set of fiber angles, due to the lack of experimental data on the building block approach to aircraft design. Moreover, several constraints in the fiber angles exist due to certain empirical rules, such as the four-contiguous-ply rule to prevent large matrix cracking. These facts make the optimization of the stacking sequences a combinatorial optimization problem with combinatorial constraints.

For optimization of the stacking sequence of the laminated CFRP composites, Genetic Algorithms (GAs) are adopted in many research programs [(3)-(7)]. Since the GAs are one of the stochastic search approaches, they do not always provide a practical optimal result and they require several parameter tuning processes to avoid any reduction in the computational performance. Narita has proposed a layer-wise optimization method for stacking sequence design [(8)].

Researchers have proposed a fractal branch and bound method (FBB) for optimizing the stacking sequence of the laminated CFRP composites [(9), (10)]. This method employs a quadratic polynomial for the response surface using the lamination parameters, such as the

*Received 9 Aug., 2010 (No. 10-0350)
[DOI: 10.1299/jcst.5.26]

buckling load, to approximate the objective functions. This method involves only low computational costs, and a practical optimal result can be obtained by means of the deterministic process in milliseconds. The FBB method is based on the discovery that plots of the feasible laminates create fractal patterns in the lamination-parameter space. Since this method is one of branch and bound approaches, tuning of the parameters is not required. This method has been successfully applied to the problem of establishing the maximization of the buckling load of a laminate [9], [10], and for determining the maximization of the flutter limit [11],[12] with constraints. The FBB method has also been applied to unsymmetrical laminates, such as composite cylinders [13].

For a practical stiffened panel made from laminated CFRP structures, the dimensions of the stiffener and panel have to be optimized simultaneously in addition to optimizing the stacking sequence. Researchers have published papers that deal with the modified efficient global optimization method using multi-objective GA [14]. In the optimizations, multiple constraints like buckling and fracture are treated as the most dangerous single constraint [15].

For the optimization to prevent the fracture of a laminated CFRP composite structure, it is difficult to obtain an approximation surrogate model [15], [16] to predict the fracture load for the check of the fracture constraints. When a quadratic polynomial was used to predict fracture of the CFRP laminate, the surrogate model provided poor estimates of this condition.

Consequently, in the present study, a new surrogate model to predict fracture is investigated. The first-ply-failure approach is adopted here, and the Tsai-Wu fracture rule is used to judge the fracture of a ply of the laminated CFRP composite. Fracture of the laminated composites is typically one of the constraints of the laminated composites. Reduction of weight is the main objective of an optimization problem for an aerospace composite component. In the present study, the maximization of the fracture load is selected as an objective function to simplify the estimate of a surrogate model to predict the fracture load. The best laminate is selected from all the possible laminates to prevent any error caused by an optimization procedure.

2. Lamination parameters

In previous papers [15], [16], a quadratic-polynomial response surface was used as a surrogate model to predict the fracture load of the target CFRP component. In these papers, lamination parameters were adopted as variables of the response surface, and the fracture load ratio against the reference loading was the response. In this section, lamination parameters are explained briefly. The lamination parameters are of two types: the in-plane lamination parameters and the out-of-plane lamination parameters.

The in-plane stiffness terms of the symmetric laminates are represented with in-plane lamination parameters V^{*i} as follows.

$$\begin{bmatrix} A_{11} \\ A_{22} \\ A_{12} \\ A_{66} \\ A_{16} \\ A_{26} \end{bmatrix} = h \begin{bmatrix} U_1 & V_1^* & V_2^* \\ U_1 & -V_1^* & V_2^* \\ U_4 & 0 & -V_2^* \\ U_5 & 0 & -V_2^* \\ 0 & \frac{1}{2}V_3^* & V_4^* \\ 0 & \frac{1}{2}V_3^* & -V_4^* \end{bmatrix} \begin{bmatrix} 1 \\ U_2 \\ U_3 \end{bmatrix}, \tag{1}$$

where h is the thickness of the laminate, U_i (i=1,...,5) are the material invariants, and V^*_I (i=1,...,4) are the in-plane lamination parameters. The material invariants are given as follows.

$$U_1 = \frac{1}{8}(3Q_{11} + 3Q_{22} + 2Q_{12} + 4Q_{66})$$
$$U_2 = \frac{1}{2}(Q_{11} - Q_{22})$$
$$U_3 = \frac{1}{8}(Q_{11} + Q_{22} - 2Q_{12} - 4Q_{66}) \quad (2)$$
$$U_4 = \frac{1}{8}(Q_{11} + Q_{22} + 6Q_{12} - 4Q_{66})$$

where

$$Q_{11} = \frac{E_L}{1 - \nu_{LT}\nu_{TL}}, \quad Q_{22} = \frac{E_T}{1 - \nu_{12}\nu_{21}}, \quad (3)$$
$$Q_{12} = \frac{\nu_{TL}E_T}{1 - \nu_{LT}\nu_{TL}}, \quad Q_{66} = G_{LT}$$

The in-plane lamination parameters are given as follows.

$$\mathbf{V} = \begin{bmatrix} V_1^* \\ V_2^* \\ V_3^* \\ V_4^* \end{bmatrix} = \frac{2}{h}\int_0^{h/2} \begin{bmatrix} \cos 2\theta \\ \cos 4\theta \\ \sin 2\theta \\ \sin 4\theta \end{bmatrix} dz, \quad (4)$$

where z is the coordinate of the thickness direction, the origin is located in the middle of the plate, and $\theta(z)$ is the fiber angle of the location of z.

The out-of-plane stiffness terms of the laminates are represented with out-of-plane lamination parameters W^*_i as follows:

$$\begin{bmatrix} D_{11} \\ D_{22} \\ D_{12} \\ D_{66} \\ D_{16} \\ D_{26} \end{bmatrix} = \frac{h^3}{12} \begin{bmatrix} U_1 & W_1^* & W_2^* \\ U_1 & -W_1^* & W_2^* \\ U_4 & 0 & -W_2^* \\ U_5 & 0 & -W_2^* \\ 0 & \frac{1}{2}W_3^* & W_4^* \\ 0 & \frac{1}{2}W_3^* & -W_4^* \end{bmatrix} \begin{bmatrix} 1 \\ U_2 \\ U_3 \end{bmatrix}. \quad (5)$$

The out-of-plane lamination parameters are defined as follows:

$$\mathbf{W} = \begin{bmatrix} W_1^* \\ W_2^* \\ W_3^* \\ W_4^* \end{bmatrix} = \frac{24}{h^3}\int_0^{h/2} z^2 \begin{bmatrix} \cos 2\theta(z) \\ \cos 4\theta(z) \\ \sin 2\theta(z) \\ \sin 4\theta(z) \end{bmatrix} dz. \quad (6)$$

When the available fiber angles are limited to 0°, 90° and ±45°, sin4θ is always zero. This means V^*_4 and W^*_4 are always zero. When the angle plies of ±45° are balanced, the total sum of sin2θ is equal to zero. This means V^*_3 is always zero. When the ±45° plies are placed within a small distance, W^*_3 becomes very small: usually the value is negligible.

3. Fracture rule

The first-ply failure rule is adopted in the present study to identify the condition of fracture of the target laminated CFRP composites. Using the selected fracture rule, the fracture load of each ply is calculated, and the smallest load in every ply is adopted as a fracture load of the target laminate. The strength of each ply is judged by means of the Tsai-Wu fracture criterion, which is shown as follows:

$$F_{11}\sigma_1^2 + 2F_{12}\sigma_1\sigma_2 + F_{22}\sigma_2^2 + F_{66}\sigma_6^2 + F_1\sigma_1 + F_2\sigma_2 = 1, \quad (7)$$

where F_{11}, F_{12}, F_{22}, F_{66}, F_1 and F_2 are defined as follows:

$$F_{11} = \frac{1}{XX'}, F_{22} = \frac{1}{YY'}, F_{66} = \frac{1}{S^2}, F_1 = \frac{1}{X} - \frac{1}{X'}, F_2 = \frac{1}{Y} - \frac{1}{Y'}, F_{12} = F_{12}^*\sqrt{F_{12}F_{22}}. \quad (8)$$

All the properties of the material strength used here are shown in Table 1. A strength factor is a proportional loading factor of the fracture from the reference load. For each stress element i (i=1,2,6), the strength factor λ is defined as follows:

$$\sigma_i^{strength} = \lambda_s \sigma_i^{applied} . \quad (9)$$

A strength factor of a laminate is defined as the minimum value of λ between all the plies in the target laminate: the first-ply failure rule is adopted here. Since the stress is proportional to the applied bending moment, λ can be applied to the bending moment without any corrections.

Table 1 Hercules AS4/3502 material properties

Property	Values
Stiffness	E_x=128GPa, E_y=11.3GPa, G_{xy}=6.00GPa, ν_{xy}=0.3
Strength	X=1154MPa, X'=838MPa, Y=51.2MPa, Y'=210MPa, S=96.5MPa, F_{12}^*=−0.5

4. Optimization problem

We now deal with the maximization of the fracture strength. Since the stacking sequence of the laminate has no relationship to the strength of the in-plane loading for symmetric laminates, the bending moment is adopted here as the only external loading. To simplify the structural analysis, a simple square CFRP plate (1 m×1 m), to which a multi-axial bending moment is applied, is adopted here as shown in Fig.1. In the target laminate, λ is the minimum value of the coefficient described in Eq. (9).

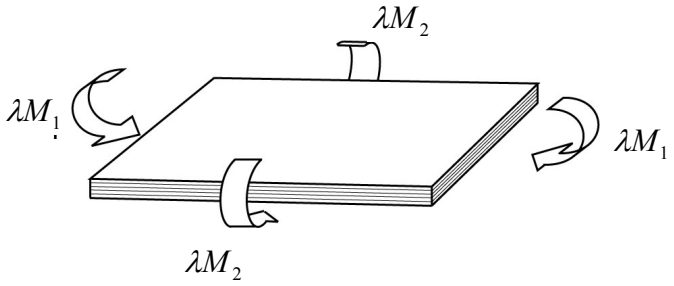

Fig.1 Configuration of the optimization target CFRP plate (1 m×1 m)

The CFRP plate has a symmetric stacking sequence of 12 plies (ply thickness =0.125 [mm]). The materials used here are AS-4/3502 composites. The applied moment is M_1=2 [N] and M_2=1 [N]. Although the CFRP plate with multi-axial pure bending is a simple problem for structural optimization, the strength of the plate with a bending moment is quite difficult to predict. The problem, therefore, is very convenient as a way to check the performance of the new surrogate model used to predict the fracture load.

Maximization of the fracture load of this square CFRP plate is performed here to check the performance of the new surrogate model. Usually, fracture is a constraint and weight reduction is the objective function for aerospace structures. In the present study, maximization of the fracture load is dealt with as an example to check the performance of the surrogate model. In searching for the highest fracture load laminate, all possible stacking sequences are searched with the surrogate model. This is to prevent the influence of the optimization tool.

5. Difficulty in predicting fracture load

This section describes why it is quite difficult to predict the fracture load of a laminated CFRP plate under a bending moment: the response of the fracture ratio is usually noisy. Let us consider the most difficult case of a pure-bending plate as shown in Fig.1. To simplify the problem, the available fiber angles are limited to 0° and 90°. The configuration of the composite plate is shown in Fig.1. In this case, bending lamination parameters W_3^* and W_4^* become zero when a symmetric laminate is used. This means that the only parameters we have to consider are the rest of the bending lamination parameters: W_1^* and W_2^*. Eq. (6) can be written as follows [9].

$$\mathbf{W} = \begin{bmatrix} W_1^* \\ W_2^* \end{bmatrix} = \sum_{k=1}^{N} \left(a_{k-1}^W - a_k^W \right) \begin{bmatrix} \cos 2\theta_k \\ \cos 4\theta_k \end{bmatrix}, \qquad a_k^W = \left(\frac{N-k}{N} \right)^3 \tag{10}$$

where N is half the number of plies. In the cases of 0°-ply and 90°-ply, the trigonometric function can be calculated as follows.

$$\begin{bmatrix} \cos 2\theta_k \\ \cos 4\theta_k \end{bmatrix} = \begin{matrix} 0° \\ \end{matrix} \begin{bmatrix} 1 \\ 1 \end{bmatrix} \quad \begin{matrix} 90° \\ \end{matrix} \begin{bmatrix} -1 \\ 1 \end{bmatrix}. \tag{11}$$

Eq. (10) and (11) imply that all the laminates are plotted on the line segment between point (1,1) and point (1-,1) in the W_1^*-W_2^* coordinate: the line of W_2^*=1 from W_1^*=-1 to W_1^*=1 as shown in Fig.2.

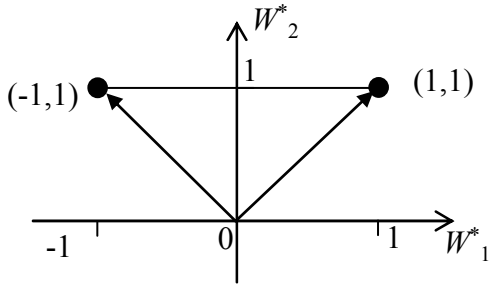

Fig.2 Line segment of W^*_1-W^*_2

Let us consider the two laminates: [0/90/90/90/0/90]s and [90/0/0/90/90/90]s. Both have the same lamination parameters (W_1^*, W_2^*) = (0.092, 1). This means the two laminates have the same bending stiffness. The strength factor λ, however, is 51.88 for [0/90/90/90/0/90]s and 63.41 for [90/0/0/90/90/90]s. These laminates have different strength factors. For the laminate of [0/90/90/90/0/90]s, the outermost 0°-ply fractured first. For the laminate of [90/0/0/90/90/90]s, the second 0°-ply fractured first.

The strength factors λ for all possible cross-ply laminates are plotted in Fig.2. The abscissa is the W_1^* (W_2^*=1 for all of the cross-ply laminates), and the ordinate is the strength factor. For the calculation of the fracture ratio λ of a laminate, the first-ply-rule (the weakest ply failure) is adopted. Open circle symbols represent the laminates in which the first ply of 0°-ply fractured; solid circle symbols represent the laminates in which the first ply of 90°-ply fractured, and the solid triangle symbols represent the laminates in which the second ply of 90°-ply fractured. The laminates near the W_1^*=1 have many 0°-plies and the laminates near the W_1^*=-1 have many 90°-plies in the lamination parameter coordinates.

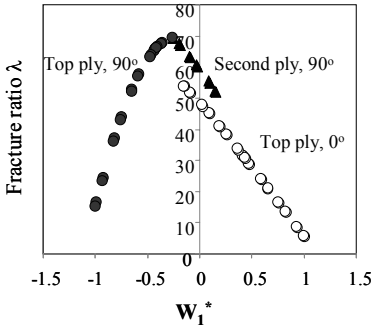

Fig.3 Fracture ratio of all possible cross-ply laminates

In Fig. 3, the strength factor is revealed not to be a single-value function for the stiffness of the laminate. This caused a large scatter of errors for the quadratic polynomial in the previous papers [15), (16)]. Figure 3 indicates that the location of the ply from the outermost ply, and the fiber angle of the ply are important variables for the regression analysis of the strength factor of the laminates. To obtain a good surrogate model, we have to consider new variables including lamination parameters, the location of the ply and the fiber angles.

6. New surrogate method

To build a new surrogate model for the fracture ratio of the laminate, several modifications were performed. Let us consider that half the number of plies of the laminate is N, and the fiber angles are limited to the small set: 0°, ±45° and 90°.

To distinguish each ply and the fiber angles, a response surface is prepared for each ply and each fiber angle. Since the ±45° plies have no different bending stiffnesses for balanced laminates, three types of response surfaces are made for each ply. Let us consider the case of the third ply. For the response surface of the third ply, three response surfaces of three fiber angles are made.

For example, a response surface of a third ply of 0° means a strength factor response surface of the laminates of [*/*/0/*/*…/*]s: the mark "*" means the ply where the fiber angle is not determined. Since there are non-determined (N-1) plies, the lamination parameters of W_1^* and W_2^* are variables for the response surface. In the present study, the in-plane lamination parameters V_1^* and V_2^* are also added to the response surface as variables for the fracture caused by in-plane loading although the in-plane loading is not applied in the present study. For the third ply, a response surface of 45° and a response surface of 90° are also made in the same way. Each ply has three response surfaces as shown in Fig.4.

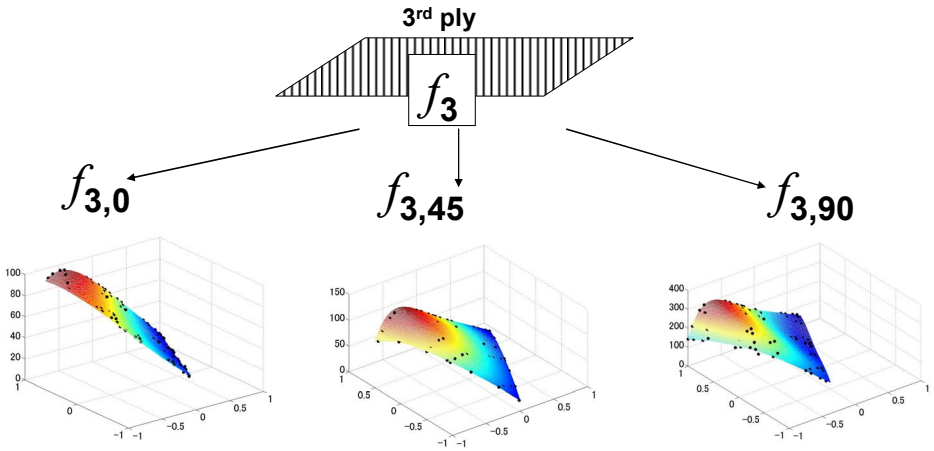

Fig.4 Schematic representation of the response surfaces of the third ply

To make the response surface, a Kriging method is adopted here. This is because the Kriging response surfaces can be applied to multiple maximum points and are robust for the design of experiments. Although there are several kinds of Kriging methods, the DACE (Design and Analysis of Computer Experiments) model is used here because it is convenient for computer calculations [17]. All the Kriging parameters are decided by using the same method as shown in a previous paper [14].

A Kriging model response surface on the basis of the DACE model that comprises a response y and variable vectors x_i (i=1,….,k) can be expressed as follows.

$$\hat{y}(\mathbf{x}) = \mu + Z(\mathbf{x}), \tag{12}$$

where all the variables are normalized from –1 to +1,and it is assumed we have n sets of analyses with n sets of responses y_j (j=1,⋯,n) and variables x_{ij} (i=1,⋯.,k and j=1,⋯,n). m is a constant value which is the averaged value of the global design space, and $Z(\mathbf{x})$ is the variable from the averaged value at point x.

$Z(\mathbf{x})$ is expressed as a realization of a stochastic process of the normal distribution of the mean value of 0. A response value y at point x is calculated as a correlation between the n sets of analysis results. The covariance matrix is given as follows.

$$Cov\left[Z(\mathbf{x}^i), Z(\mathbf{x}^j)\right] = \sigma^2 \mathbf{R}\left[R(\mathbf{x}^i, \mathbf{x}^j)\right], \tag{13}$$

where R means the correlation matrix, and the element $R(x_i,x_j)$ is a value of the Gaussian correlation function between point x_i and point x_j. In the present study, a distance between the two points of each variable may not be expressed on a similar scale. This suggests the use of a scaled distance by means of multiplexing a constant with a distance, and the Gaussian correlation function can be written as follows.

$$R(\mathbf{x}^i, \mathbf{x}^j) = \exp\left[-\sum_{m=1}^{k} \eta_m \left| x_m^i - x_m^j \right|^2\right], \tag{14}$$

where η_m ($\eta_m \geq 0$, m=1,...,k) are unknown correlation parameters. To make a DACE model, the unknown parameters η_m must be obtained. In Eq.(14), x_m^i and x_m^j are the mth elements of the position vectors x_i and x_j. The value of the correlation function means the degree of influence between two points on the response. A higher value means a higher degree of influence; the point is affected by the points located around the point. Since each design variable has a different scale to the correlation parameter, the strength of the effect of the correlation parameter can be controlled by means of the unknown value of η_m.

The expected response at a point x can be calculated as follows.

$$\hat{y}(\mathbf{x}) = \hat{\mu} + \mathbf{r}^T \mathbf{R}^{-1}(\mathbf{y} - \mathbf{1}\hat{\mu}), \tag{15}$$

where $\hat{\mu}$ is an estimator of μ : $\mathbf{y}$ is a column vector that has n elements of responses at the n sample points: $\mathbf{1}$ is a column vector whose elements are all 1 ($[1,...,1]^T$) and $\mathbf{r}$ is a column vector that has values of the correlation function between the target point and the other sample points.

$$\mathbf{r}(\mathbf{x}) = \left[R(\mathbf{x}, \mathbf{x}^1), R(\mathbf{x}, \mathbf{x}^2), \cdots, R(\mathbf{x}, \mathbf{x}^n)\right]^T. \tag{16}$$

Assume that the values of η are given, $\hat{\mu}$ and the variance of $\hat{\mu}$ ($\hat{\sigma}^2$) can be calculated as follows.

$$\hat{\mu} = \frac{\mathbf{1}^T \mathbf{R}^{-1} \mathbf{y}}{\mathbf{1}^T \mathbf{R}^{-1} \mathbf{1}}, \tag{17}$$

$$\hat{\sigma}^2 = \frac{(\mathbf{y} - \mathbf{1}\hat{\mu})^T \mathbf{R}^{-1} (\mathbf{y} - \mathbf{1}\hat{\mu})}{n}. \tag{18}$$

The only problem left is how to obtain the parameter η of the DACE mode. For the estimate of the values of η, a log likelihood function is adopted.

$$Ln(\boldsymbol{\eta}) = -\left[n \ln(\hat{\sigma}^2) + \ln|\mathbf{R}|\right]/2, \tag{19}$$

where $\hat{\sigma}$ and $\mathbf{R}$ are functions only of $\boldsymbol{\eta}$. The correlation parameter η is obtained by means of the maximization of the log likelihood function. In this problem, the number of unknown values is k. The method is described in references [14), (17].

To make the Kriging response surface, we have to do a lot of computation to obtain the fracture ratios of the various laminates. It is impossible to perform a new design of experiments to make each response surface. A newly developed design of experiments using Latin Hypercube Sampling, therefore, is proposed for the all response surfaces in the present study. The sampling number is set to a multiple number of three: three implies equal configurations of 0°, 45° and 90° plies and the available fiber angles. In the present study, an odd occurrence of an angle ply fiber angle means the minus angle, an odd occurrence of 45° from the outermost ply means -45° in this study. Let us consider the case of sampling number 9.

First, a list of stacking sequences is prepared as shown in Table 2. From line 1 to line 3, all the fiber angles are set to 0°, all the fiber angles from line 4 to line 6 are 45° and all the fiber angles from line 7 to line 9 are 90° as shown in Table 2. After this preparation, the fiber angles of each row are swapped at random in the target row. After this swapping, the stacking sequences at random fiber angles are obtained as shown in Table 3. In the table, the second appearance of 45° means -45° to obtain balanced angle ply laminates. When the total number of plies of 45° is odd, there is only one excessive 45°-ply near the middle of the laminates. Although the excessive 45°-ply results in an un-balanced laminate, the un-balanced effect is very small because the excessive ply locates near the middle of the laminate for bending stiffness. For in-plane stiffness, the effect of only one excessive ply is too small for a laminate of a large number of plies. The effect of excessive ply is, therefore, neglected. After making this stacking sequence set, analyses of the fracture ratio are performed for all the laminates.

Table 2 Preparation of sample stacking sequences

	1st ply	2nd ply	.....	Nth ply
No.1	0	0	.....	0
No.2	0	0	.....	0
No.3	0	0	.....	0
No.4	45	45	.....	45
No.5	45	45	.....	45
No.6	45	45	.....	45
No.7	90	90	.....	90
No.8	90	90	.....	90
No.9	0	90	.....	90

Table 3 Obtained stacking sequences

	1st ply	2nd ply	.....	Nth ply
No.1	0	0	.....	45
No.2	45	90	.....	0
No.3	0	45	.....	45
No.4	90	0	.....	0
No.5	45	45	.....	90
No.6	0	90	.....	45
No.7	45	0	.....	90
No.8	90	90	.....	0
No.9	0	45	.....	90

Table 4 Sorted laminates that have 0°-ply in the second ply

	1st ply	2nd ply	.....	Nth ply
No.1	0	0	.....	45
No.2	90	0	.....	0
No.3	45	0	.....	90
No.4	0	45	.....	45
No.5	45	45	.....	90
No.6	0	45	.....	90
No.7	45	90	.....	0
No.8	90	90	.....	0
No.9	0	90	.....	45

Let us consider the case where we want to obtain a response surface of the second ply for the fiber angle of 0°. As we prepared three plies that have 0°-ply in the second ply as shown in Table 2, we have three laminates that have 0°-ply in the second ply as shown in Table 3. Using the three laminates, we can calculate the response surface of the second ply for the fiber angle of 0°. In the same way, we can calculate the other response surfaces with this table.

When half the number of plies is N (total number of plies is $2N$), the total number of calculations is $3\times N$. The design of the experiments significantly reduces the number of calculations for making all the response surfaces.

From this design of experiments, we can obtain all the response surfaces of all plies and of all fiber angles. When we want to obtain the fracture ratio of a laminate, we have to calculate these response surfaces.

Let us consider the case of the laminate of [0/90/45/0/-45/90]s We can start the calculation from the top ply of 0°. Since the fiber angle of the top ply is fixed to 0°, we can calculate the fracture ratio of the top ply of 0°. As we know the other fiber angles, we can obtain the lamination parameters. This enables us to calculate the fracture ratio using the response surface. For the other plies, we can calculate the fracture ratios similarly. From this process, we can obtain all the fracture ratios of all the plies. In this case, we can obtain six fracture ratios. After this, we have to search for the minimum fracture ratio from this list of the fracture ratios. The minimum fracture ratio on the list is selected as the true fracture ratio of the laminate.

7. Results and discussion

As a comparison, the fracture ratios of the composite plate (N=12 plies) of Fig.1 are approximated by means of the normal quadratic polynomial response surface. For the quadratic polynomial response surface to predict the fracture ratio, four lamination parameters are adopted as variables. Since the total number of coefficients of the quadratic polynomial response surface is 15 (=1+4+4+4×3/2), a random selection of 20 laminates is used to make the response surface of the quadratic polynomial. Since the laminate is a symmetric laminate of 12 plies (half number of plies is 6), the total number of possible laminates is 3^6=729 for the laminates comprising of 0°, 90° and 45° (±45°).

The results of the previous surrogate model of the quadratic polynomial for all of the 729 laminates are plotted in Fig.5. In Fig.5, the abscissa is the true fracture ratio of the laminates and the ordinate is the estimated fracture ratio of the laminate. The solid diamond symbols refer to the estimated results of the laminates. The plots located on the diagonal line mean the estimates are exact. As shown in Fig.5, the estimates show large estimation

errors. As mentioned in Section 5, this error comes from the multi-value function when we use only lamination parameters as variables.

Figure 6 shows the estimate results of the new surrogate model using the Kriging response surface made from 36 analyses: 12 analyses are used to make one Kriging response surface; the total number of response surfaces is 18=6 (number of plies) ×3 (number of fiber angles). The abscissa is the true fracture ratio of the laminates and the ordinate is the estimated fracture ratio. Open circle symbols are the fracture ratios of the practical laminates. Plots on the diagonal line mean the estimate is excellent. Therefore, for the comparison of the two response surfaces, the coefficient of multiple determination R^2 to the diagonal line is calculated here. For the quadratic polynomial response surface, R^2=0.60, and for the new Kriging response surface, R^2= 0.96. The higher value means estimations are excellent. The results in Fig.6 show the estimates are excellent when they are compared with the results of Fig.5.

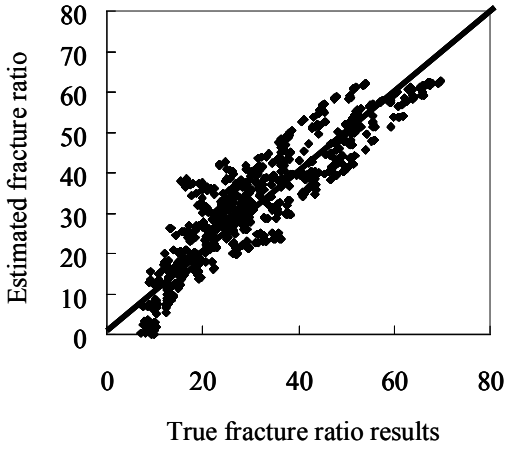

Fig.5 Results of quadratic polynomial response surface

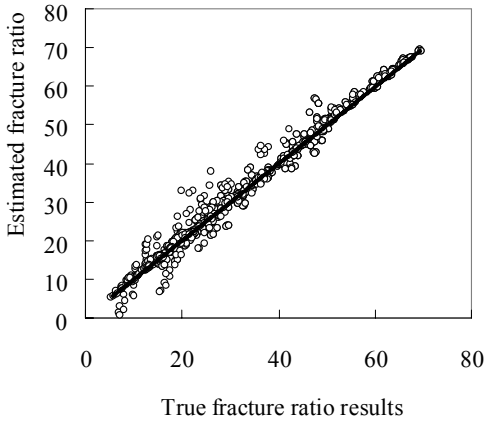

Fig.6 Results of Kriging response surface of the proposed method

Since the fracture ratio is obtained using the surrogate model, stacking sequence optimization to maximize the fracture ratio was carried out. All the possible laminates were checked using the surrogate model. The obtained optimal stacking sequence was $[90/0/90/0/90/0]_s$ and the fracture ratio of the laminate was λ_{max}=69.3. The true optimal laminate was searched for and the stacking sequence was $[90/0/90/0/90/90]_s$: the true optimal fracture ratio was λ_{max}=69.6. The difference was only 0.4 %. This small error is acceptable for practical design. From this result, the proposed Kriging model is appropriate for the surrogate model of the fracture strength of bending loading for laminated CFRP. If

we do the design of the experiments for each response surface, we have to do 216=18×12 analyses. The present method significantly reduces number of analyses.

8. Concluding remarks

The present paper deals with a new surrogate model for approximating the fracture strength of laminated composites. The results obtained were as follows.

(1) The difficulty of the mechanism for making a surrogate model was shown here: the multi-value function for approximating the fracture ratios of laminated composites causes the problem.

(2) A new surrogate model using a Kriging was proposed: a Kriging regression model was made for each ply and for each fiber angle.

(3) The design of experiments using the Latin Hyper Cubic for the new surrogate model was proposed.

References

(1)M. Miki, Design of Laminated Fibrous Composite Plates with Required Flexural Stiffness, *ASTM STP*, 846 (1985), pp.387-400.

(2)H. Fukunaga and G. Vanderplaats, Stiffness Design Method of Symmetric Laminate Using Lamination Parameters, *AIAA J.* Vol. 30, No. 11 (1992), pp.2791-2795.

(3) R. Le Riche and R. T. Haftka, Optimization of Laminate Stacking Sequence for Buckling Load Maximization by Genetic Algorithm, *AIAA J.*, Vol. 31, No. 5 (1993), pp.951-956.

(4) B .Liu, R.T. Haftka, M. Akgün and A. Todoroki, Permutation Genetic Algorithm For Stacking Sequence Design Of Composite Laminates, *Computer Methods in Applied Mechanics and Engineering,* Vol. 186, No. 2-4 (2000), pp.357-372.

(6) J.H. Park, J.H. Hwang, , C.S. Lee, and W. Hwang, Stacking sequence design of composite laminates for maximum strength using genetic algorithms, *Composite Structures*, Vol. 52, No. 2 (2001), pp.217-231.

(7) M.H. Cho and S.Y. Rhee, Layup Optimization Considering Free-Edge Strength and Bounded Uncertainty of Material Properties, *AIAA J.*, Vol. 41, No. 11 (2003), pp.2274-2282.

(8) Y. Narita, Layerwise optimization for the maximum fundamental frequency of laminated composite plates, *Journal of Sound and Vibration*, Vol. 263 (2003), pp.1005-1016.

(9) Y. Terada and A. Todoroki and Y. Shimamura, Stacking Sequence Optimizations Using Fractal Branch and Bound Method for Laminated Composites, *JSME International J., Series A*, Vol. 44, No. 4 (2001), pp.490-498.

(10) A. Todoroki and Y. Terada, Improved Fractal Branch and Bound Method for Stacking Sequence Optimizations of Laminated Composite Stiffener, *AIAA J.*, Vol. 42, No. 1 (2004), pp.141-148.

(11) Y. Hirano and A. Todoroki, Stacking sequence optimizations for composite laminates using fractal branch and bound method (Application for Supersonic Panel Flutter Problem with Buckling Load Condition), *Advanced Composite Materials*, Vol. 13, No. 2 (2004), pp.89-107.

(12) Y. Hirano and A. Todoroki, Stacking-Sequence Optimization of Composite Delta Wing to Improve Flutter Limit Using Fractal Branch and Bound Method, *JSME Int. J., Series A*, Vol. 48, No. 2 (2005), pp.65-72.

(13) R. Matsuzaki and A. Todoroki, Stacking Sequence Optimization Using Fractal Branch and Bound Method for Unsymmetrical Laminates, *Composite Structures*, Vol. 78, No. 4 (2007), pp. 537-550.

(14) Akira Todoroki and Masato Sekishiro, Modified Efficient Global Optimization for a Hat-stiffened Composite Panel with Buckling Constraint, *AIAA J.*, Vol. 46, No. 9 (2008), pp.2257-2264.

(15) Akira Todoroki & Masato Sekishiro, Optimization of Blade Stiffened Composite Panel

under Buckling and Strength Constraints, *Journal of Computational Science and Technology, JSME* Vol. 2, No. 1 (2008), pp.234-245.

(16) Akira Todoroki and Masato Sekishiro, Stacking Sequence Optimization to Maximize Buckling Load of Blade-Stiffened Panels with Strength Constraints using the Iterative Fractal Branch and Bound Method, *Composite B* , Vol. 39, No. 5 (2008), pp.842-850.

(17) W.J. Welch, R.J. Buck, J. Sacks, H.P. Wynn, T.J. Mitchell, and M.D. Morris, "Screening, Predicting, and Computer Experiments," *Technometrics*, Vol. 34, No. 1 (1992), pp.15-25.